Isı Bilimi ve Tekniği Dergisi, 29, 2, 67-73, 2009
J. of Thermal Science and Technology

ISSN 1300-3615

THE EFFECTS OF LASER ENERGY DEPOSITION ON SUPERSONIC CAVITY FLOW

Selin ARADAG[*], Hong YAN[+], Doyle KNIGHT[&]
[*]TOBB University of Economics and Technology , Department of Mechanical Engineering
06560, Ankara, saradag@etu.edu.tr
[+]Wright State University, Department of Aerospace Engineering, Dayton, Ohio, USA
[&]Rutgers University, Department of Mechanical and Aerospace Engineering, New Brunswick, NJ, USA

(Geliş Tarihi: 16. 03. 2009, Kabul Tarihi: 14. 05. 2009)

Abstract: The study examines the capability for reduction of the resonant pressure fluctuations in supersonic flow over an open rectangular cavity using repetitively pulsed energy deposition, computationally. The simulations are performed for the cases both with and without energy deposition for the unsteady flow over a three-dimensional cavity at a free stream Mach number of 1.5. The Reynolds-averaged compressible time dependent Navier Stokes equations in three dimensions are solved using the flow solver GASPex. The k-ω turbulence model is used. A Gaussian temperature profile is utilized to model the energy pulse assuming the density within the spot is initially uniform. The results indicate that energy deposition reduces the pressure fluctuations changing the flow structure within the cavity.
Keywords: Computational fluid dynamics, supersonic cavity, laser energy deposition, flow control, open cavity

LAZER ENERJİSİNİN SESÜSTÜ KAVİTELERDEKİ AKIŞ ÜZERİNE ETKİLERİ

Özet: Bu çalışma, açık dikdörtgensel kaviteler üzerindeki basınç dalgalanmalarının lazer enerjisi ile azaltılmasının mümkün olup olmadığını araştıran sayısal bir çalışmadır. Simülasyonlar, enerji gönderilen ve gönderilmeyen iki ayrı durumda üç boyutlu bir kavite üzerindeki zamana bağlı değişen Mach sayısı 1.5 olan sesüstü akış için gerçekleştirilmiştir. Sıkıştırılabilir zamana bağlı Reynolds-ortalamalı Navier Stokes denklemleri üç boyutta GASPex adlı kod kullanarak çözümlenmiştir. Türbülans modeli olarak k-ω kullanılmıştır. Lazer enerjisini modellemek için Gauss sıcaklık profili kullanılmış, enerjinin gönderildiği noktadaki yoğunluğun başlangıçta uniform olduğu kabul edilmiştir. Çalışmada elde edilen sonuçlara göre, lazer enerjisi kavite içindeki akış yapısını değiştirerek, basınç dalgalanmalarını azaltmaktadır.
Anahtar Kelimler: Hesaplamalı Akışkanlar Dinamiği, sesüstü kavite, laser enerjisi gönderimi, akış kontrolü, açık kavite

NOMENCLATURE

D:	Cavity depth
E:	Total energy deposited
L:	Length of cavity
M:	Mach number
Re:	Reynolds number
SPL:	Sound pressure level
U:	Free-stream velocity
W:	Width of the cavity
Δt:	Time step
f_m:	Rossiter frequency
t_R:	Rossiter period
t_f:	Final time
t_i:	Initial time
δ:	Boundary layer thickness
ε:	Non-dimensional energy deposition parameter

INTRODUCTION

High speed flows over open cavities can produce complex unsteady flowfields that are physically important and become a practical concern in aerospace applications. These complex unsteady flowfields include not only the small-scale pressure fluctuations typical of turbulent shear flows but also a significant resonance, the frequency and amplitude of which depend on the cavity geometry and external flow properties.

Supersonic flow past a cavity has numerous applications in store carriage and release. Internal carriage of stores is used for supersonic aircraft in order to minimize aerodynamic drag, aerodynamic heating and radar signature. It also provides several advantages including enhanced maneuverability and expanded flight envelope. However, the intense pressure fluctuations and significant resonant acoustic modes that are generated by the flow past an open cavity at supersonic speeds can damage the structure of the aircraft and stores and impede successful store release. This severe acoustic environment within the cavity can also represent a potential hazard to sensitive instrumentation.

The flowfield structure within a rectangular cavity can be categorized into two main types, namely open and closed cavity configurations depending on the cavity streamwise length to depth ratio L/D as illustrated in Fig. 1. The flow in the shallow cavity where the depth to length ratio is small is called closed cavity flow, whereas the flow for the deep cavity is called open cavity flow. In the open cavity, the free shear layer attaches on the rear face, thereby forming a single recirculation region. In the closed cavity, the shear layer reattaches on the cavity floor, and the flowfield is a combination of a backward and forward facing step.

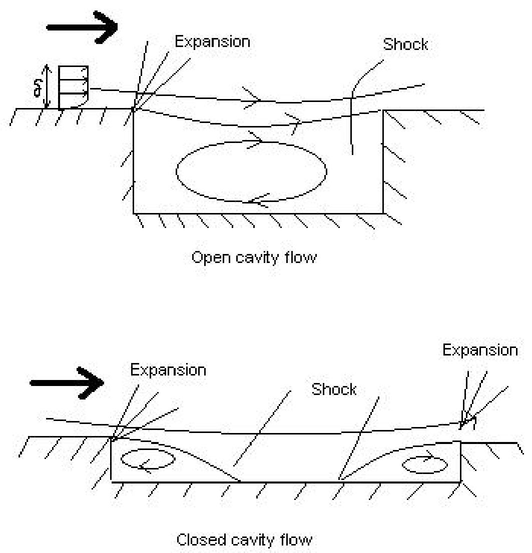

Figure 1. Types of Cavity Flows

Numerous research studies on supersonic cavity flow have been conducted. A review of the early work in subsonic and supersonic flow past a cavity was made by Charwat et al (1961). Rockwell and Naudascher (1978) reviewed the field and categorized flow types. Perng (1996) presented a more recent review. Rossiter (1964) proposed an empirical formula for predicting the frequencies of the pressure oscillation modes, based on his shadowgraph studies of subsonic and transonic shallow cavities. Modes can be predicted well by improved versions of his formula, but any simple method does not exist for predicting the fluctuation amplitudes. Heller and Bliss (1975) modified Rossiter's formula for the prediction of mode frequencies. Bauer and Dix (1991) present a simple analytical method, which uses the modified Rossiter equation to predict frequencies.

Several experimental and computational studies have also been performed on cavity flow. Leu and Dolling (1997) conducted a series of tests on high speed, rectangular, open cavity flows with store release and shock impingment. They measured fluctuating surface pressure in a cavity, where L/H=3 at Mach 5. Their results show that the cavity flow field remains essentially the same whether a store is placed inside the cavity or not. Unalmis et al (1999, 1998) made planar laser imaging and fluctuating pressure measurements in a Mach 5 cavity flow, with varying L/D. They concluded that the acoustical phenomena inside the cavity do not have much effect on the shear layer dynamics, which suggests a weak shear layer/acoustics coupling in the current cavity flow, resulting in purely acoustic modes. Hankey and Shang (1979) predicted the pressure oscillations for supersonic flow over an open cavity by numerically solving the two dimensional unsteady Navier Stokes equations for Mach 1.5 configuration of Heller and Bliss (1975) and obtained good agreement for both the magnitude and frequency of the lowest order modes. Rizzetta (1988) performed a three dimensional unsteady RANS simulation at a free stream Mach number of 1.5 and observed good agreement with experimental data with which comparisons were made in terms of mean static pressure and overall acoustic sound pressure levels within the cavity. Shih et al (1994) developed a numerical procedure for the simultaneous implicit solution of the coupled k-ε and Navier-Stokes equations for compressible viscous flows and compared the results with experiments and other computations.

A variety of active and passive control techniques have been investigated to reduce the sound pressure level (SPL) associated with the resonant acoustic fluctuations. In passive control approach, the cavity is modified in some way, such as a mounted device. Passive control methods are inexpensive, simple and effective in suppressing the oscillations. However, the performance of the cavity in time varying conditions may be worse than that without control, since passive control uses permanent devices. Active control methods can continuously change to adapt to varying flow conditions. Examples of active and passive control are the studies performed by Lamp and Chokani (1997) and Stallings et al (1994). Lamp and Chokani (1997) performed computations on cavity flows with suppression using jet blowing. Stallings et al (1994) investigated the effect of passive venting on static pressure distributions in cavities. Zheltovodov et al (1991) also studied supersonic flow over rectangular cavities and methods of flow control. Aradag et al (2004) studied the effects of laser energy deposition on supersonic cavities computationally and Lazar et al (2008) studied the same cavity configuration experimentally.

OBJECTIVES

The aim of this research is to simulate supersonic turbulent flow past an open rectangular cavity, and to examine the capability of pulsed energy deposition to reduce the resonant pressure levels in the cavity.

STATEMENT OF THE PROBLEM

The coordinate system and the configuration that are considered are given in Fig 2. The geometry represents one of the cases of the experimental data of Kaufman et al (1983). The length to depth ratio for the cavity, L/D is 5.07, the length to width ratio, L/W is 1.90. The other principal parameters are the free stream Mach number of 1.5 and the Reynolds number of 1.09 10^6 based on the free stream conditions and the cavity length, L. The free stream static temperature is 218 K and the free stream total pressure is 66.4 kPa. The ratio of the boundary layer thickness immediately upstream of the separation point to the cavity depth δ/D is 0.213.

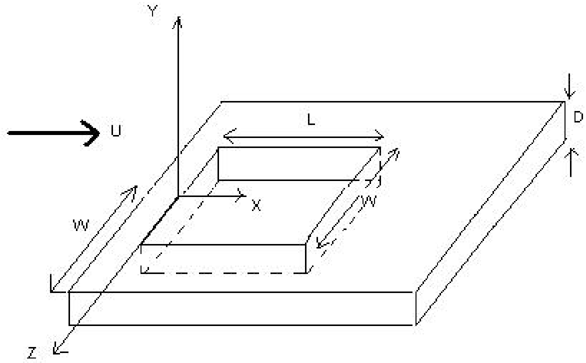

Figure 2. Cavity Configuration

A periodic pulsed energy input of 1.0 mJ is given to the leading edge of the cavity to simulate the energy deposition by laser, which corresponds to a dimensionless energy parameter, ε=4.0, non-dimensionalized using static enthalphy. The dimensionless energy deposition parameter (Knight et al, 2003) is defined as

$$\epsilon = \frac{Q_T}{\rho_\infty c_p T_\infty V + \rho_\infty c_p T_\infty U_\infty A \tau_e} \tag{1}$$

The numerator is the amount of energy deposition in V in time τ_e. The denominator is the sum of two terms. The first term is the static enthalphy in region V at the beginning of the energy pulse. The second term is the static enthalphy flux through the cross sectional area A during the characteristic timescale of the energy deposition τ_e (Knight et al, 2003). The second term is neglected in this study since the energy pulse is assumed instantaneous.

A spherically symmetric initial temperature distribution is proposed to model each energy pulse (e.g., by laser) assuming the energy is added instantaneously at constant volume (Yan et al, 2003). Therefore the density is constant and an ideal gas is assumed. The temperature variation using a Gaussian profile can be written as:

$$\triangle T = T_0 e^{-r^2/r_0^2} \tag{2}$$

where the peak temperature variation, ΔT_0 is determined by the total energy deposited, E, which is 1.0 mJ. The energy deposited is given by

$$E = \int_0^{2\pi} \int_0^{\pi} \int_0^{\infty} r^2 \sin\theta \rho_\infty c_v \triangle T dr d\theta d\phi \tag{3}$$

where c_v is the specific heat at constant volume. Substituting (2) into (3) and integrating, we obtain

$$\triangle T_0 = \frac{E}{\pi^{3/2} r_0^3 \rho_\infty c_v} \tag{4}$$

where r_0 is related to the assumed initial radius R_0=0.9 mm of the energy pulse obtained from the perturbation focal volume $V_0 = 4/3\pi R_0^3$ and set to be $R_0/2$. From Eq. (2), ΔT will reach 2% of ΔT_0 at $r=R_0$. The ratio of the energy pulse radius to incoming boundary layer thickness R_0/δ is 0.177.

Despite its inherent simplicity, the energy deposition model provides an accurate prediction of the flowfield generated by a laser pulse outside of the laser focal volume and its immediate neighborhood. The model was validated by comparison with Filtered Rayleigh Scattering measurements (Yan et al, 2003).

NUMERICAL METHODOLOGY

The flow solver is GASPex Version 4.1.0+ (1996) which is a structured multiblock CFD solver that is applicable to compressible flow fields approximately at Mach 0.2 or higher. It solves the Reynolds-averaged compressible time dependent Navier Stokes equations in three dimensions, utilizing a finite volume spatial discretization in which the state variables are stored at the cell centers. Inviscid fluxes are modeled using third order upwind Van Leer scheme. The computations are second order accurate both in time and space.

The turbulence model is k-ω, which is a two-equation model. This turbulence model is widely used to simulate incompressible and compressible flows. In this model, transport equations for the turbulent kinetic energy k and a second parameter ω (the rate of dissipation of energy per unit volume and time) are solved (Wilcox, 1993). The Sutherland viscosity law is employed together with the ideal gas relation in the computations.

The configuration is symmetric about the cavity centerline, so the computational domain is half of the physical domain. Inflow boundary conditions were obtained from the numerical solution of the two-dimensional steady flow equations over a flat plate at the free stream conditions of the cavity flow, using program EDDYBL (Wilcox, 1993). This computation employed a finer grid distribution than that is used for the cavity computation, so a cubic spline interpolation was used to interpolate the results to the cavity flow computational domain. The flat plate computational domain extended from the leading edge of the cavity experimental configuration (x = -1.526L) to the forward bulkhead. Results of this solution at x = -0.249L established upstream profiles of the dependent variables at all spanwise locations. The incoming boundary layer thickness matched the experiment. On the solid boundaries, the no-slip conditions

$$u = v = w = 0 \tag{5}$$

was employed along with

$$\frac{\partial p}{\partial n} = 0 \tag{6}$$

$$T = T_{aw} \tag{7}$$

where the isothermal wall temperature was taken as the adiabatic wall temperature that was calculated to be 304.8 K and n is the direction normal to the surface. The solid wall boundary conditions for k and ω are

$$k = 0 \tag{8}$$

$$\omega = \frac{\rho u_*^2 r}{\mu_l} \tag{9}$$

where u_* is the wall shear velocity, ρ is the local density, μ is the local laminar viscosity and r is a parameter related to the non-dimensional roughness. For the outflow and upper computational boundaries, first order extrapolation was used. On the centerline, symmetry conditions were satisfied. Above the cavity mouth, the initial conditions were taken as the inflow conditions. Inside the cavity, wall values were assigned.

The computational domain has a nonuniform Cartesian mesh consisted of two zones that are the inside and outside of the cavity. The total number of cells in the inside zone are 95 X 54 X 35, and 177 X 62 X 70 in the outside zone, in the x, y, z directions, respectively. Grid clustering was employed at several places in the domain. Exponential stretching was used for this purpose with Δn_{min}^+ of 1.0, at the solid boundaries. The minimum grid spacing employed is: $\Delta x_{min}/L = \Delta y_{min}/L = \Delta z_{min}/L = 0.00004$. Both within and outside the cavity, the y value is stretched from the minimum value at the mouth of the cavity to a constant value of 0.02, over the first 27 grid points. The first 12 z-grid points have a uniform spacing of Δz/L=0.02, starting from the cavity symmetry plane. Stretching takes place along both sides starting from the centers of the y-z planes of the computational domain up to 27 z-grid points. ICEMCFD software was used for the generation of structured grid. At the inflow boundary, there are approximately 24 points within the boundary layer. The extent of the simulation domain was -0.24865<x/L< 1.5, -1.0< y/D<4.0, 0<z/(W/2)<2.0.

The unsteady solutions were obtained using the implicit dual step method. The time increment, Δt is 1μs corresponding to 0.0012 non-dimensional time, non-dimensionalized by the fundamental Rossiter period. (t_R) The Rossiter period is the inverse of Rossiter frequency which is defined as

$$f_m = \frac{mU}{L(M_o + K^{-1})} \tag{10}$$

where μ is the number of waves or mode number, L is the cavity length, U is the free stream velocity. M_0, the ratio of free stream velocity to the stagnation speed of sound which is given by $a_0 = \gamma$ R T_0, is calculated to be 1.246. K is taken as 0.55 for this cavity configuration (Hankey and Shang, 1979).

For the computations, one of the Beowulf computer clusters of Rutgers University (mphase) was used. The core of the mphase cluster consists of 60 dual and single processor Linux machines. A total of 32 processors in this cluster were used for the computations. Each time step takes 148 seconds with 32 processors. Each processor uses 500 MB of memory. The CPU time per time step per cell is 6miliseconds.

RESULTS

The simulations for unsteady supersonic flow past an open rectangular cavity with and without energy deposition were conducted for one of the test cases of the experimental study by Kaufman et al. and the results were compared with the experimental data along the cavity centerplane, for the case without energy deposition.

The flowfield solution was integrated in time starting from the initial profiles. After 1000 μs, it was judged that the flow field was free of initial transients and had reached a periodic state at which the oscillations were self-sustaining. This time corresponds to 1.2 fundamental Rossiter periods. Then, computations were performed for an additional 12 Rossiter periods, corresponding to 10,000 time steps, to compare the computed fundamental Rossiter period with the theoretical value.

The pressure fluctuations at a location, on the downstream face at the centerplane, at y/D=0.6 where y is measured from the cavity floor, are shown in Fig 3 Even though the mean pressure value is not much higher than the free stream static pressure, peak pressures can be even 2.5-3 times the freestream value.

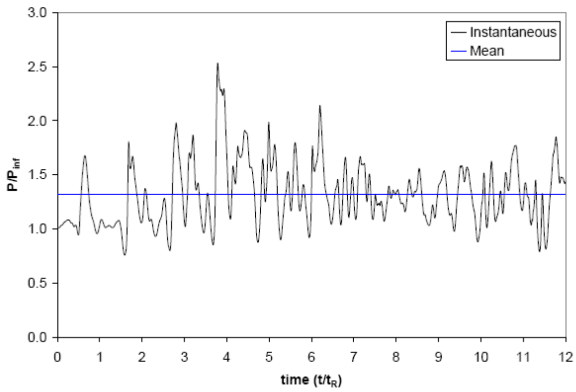

Figure 3. Pressure Fluctuations on centerplane at y/D=-0.4

In Fig. 4, the acoustic streamwise pressure distribution on the cavity floor is given as the Sound Pressure Level (SPL), in decibels, defined as:

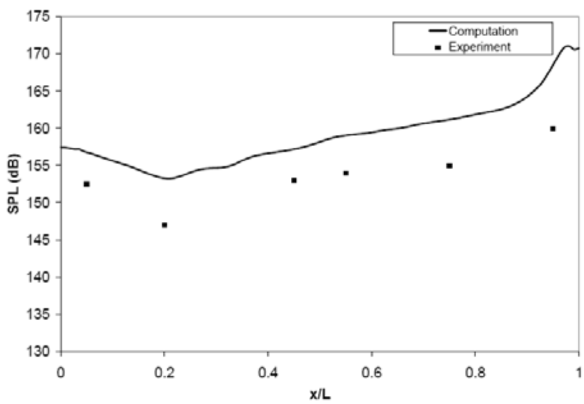

Figure 4. SPL Distribution on Cavity Floor (Without energy deposition)

$$SPL = 10\log_{10}(\frac{\bar{p}^2}{q^2}) \tag{11}$$

where

$$\bar{p}^2 = \frac{1}{(t_f - t_i)}\int_{t_i}^{t_f}(p-\bar{p})^2 dt \tag{12}$$

and

$$\bar{p} = \frac{1}{(t_f - t_i)}\int_{t_i}^{t_f} pdt \tag{13}$$

and q is the sound pressure reference level of 2 10^{-5} Pa and t_f-t_i (Final time-initial time)=12t_R. The computations are within 10 dB of experimental results.

The first energy pulse of 1.0 mJ, which corresponds to a dimensionless energy parameter of 4.0, was deposited to the flow after 12 Rossiter periods. An energy input of same amount was added at the beginning of each fundamental Rossiter period. The effects of the amount, location and frequency of energy deposition was not tested. Energy is only deposited periodically at the beginning of each Rossiter period. Computations were performed for 12 Rossiter time periods after the first energy deposition.

Pressure fluctuations at the experimental measurement location at the aft bulkhead after energy deposition for 12 Rossiter periods is shown in Fig. 5. Energy deposition changes the pressure distribution as seen in the figure. It decreases the peak pressures compared to the no energy deposition case (Fig. 3), whereas the mean pressure remains almost the same.

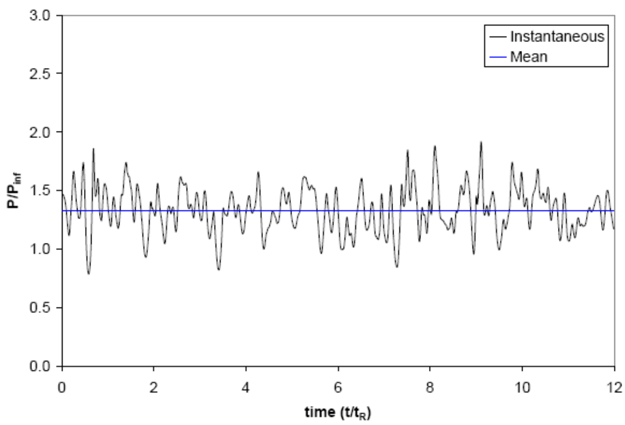

Figure 5. Pressure Fluctuations on centerplane at y/D=-0.4 after energy deposition

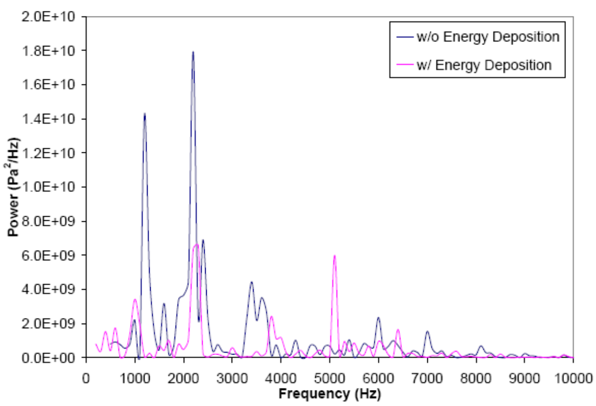

Figure 6. Power Spectrum

The power spectrum versus frequency graph which shows the fundamental pressure frequencies in the flow, obtained from pressure histories is given for the energy deposition case, after 12 Rossiter periods, on the same figure with the case before energy deposition in Fig. 6. The peak powers decrease after 12 Rossiter periods with pulsed energy deposition at the beginning of each Rossiter period. The peak values of the power spectrum are at almost the same frequencies as the case without energy deposition.

The acoustic streamwise pressure distribution on the cavity floor at the centerplane, is given as SPL in decibels in Fig. 7 after energy deposition for 12 Rossiter periods. The pressures decrease uniformly along the cavity floor after energy deposition.

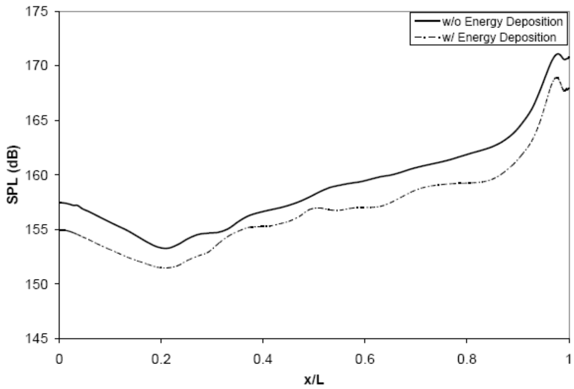

Figure 7. Pressure Distribution on Cavity Floor before and after Energy Deposition

In Fig. 8 and Fig. 9, sound pressure level distributions are shown on the forward and aft bulkheads, at the centerplane, after 12 Rossiter periods. They also decrease uniformly after energy deposition. In Fig. 8, at the forward bulkhead, the location where energy is deposited remains the only position where the SPL values do not decrease, which is reasonable since the pressures are increased at the energy deposition location.

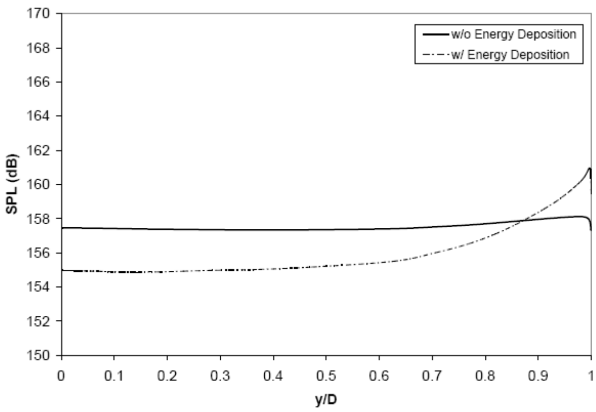

Figure 8. Pressure Distribution on Upstream Face of the Cavity before and after Energy Deposition

Energy deposition is continued for an additional 10 Rossiter periods to examine the convergence of the power spectrum at the experimental measurement location. The power spectrum does not converge to a single state when the computations are continued for several Rossiter periods. The peak powers of the power spectrum for the first and second Rossiter modes t/t_R since the beginning of energy deposition are shown in Fig. 10. The peak power for the fundamental Rossiter frequency in the absence of energy deposition is also shown. It is clearly seen from Fig. 10 that the peaks of the power spectrum change after each Rossiter period, if we continue the computations by depositing energy at the beginning of each Rossiter period. Although the peak powers are changing after deposition of energy, after each Rossiter period, they still remain smaller than the one before energy deposition.

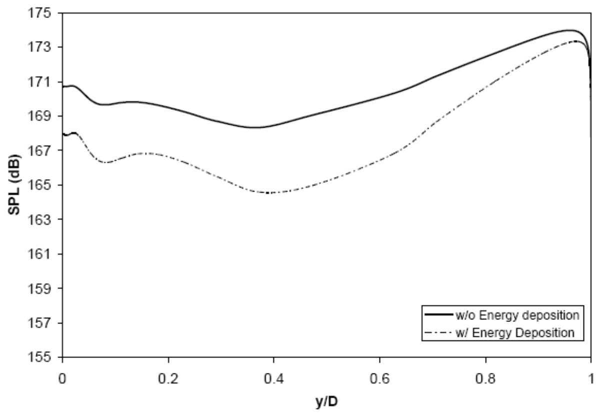

Figure 9. Pressure Distribution on Downstream Face of the Cavity before and after Energy Deposition

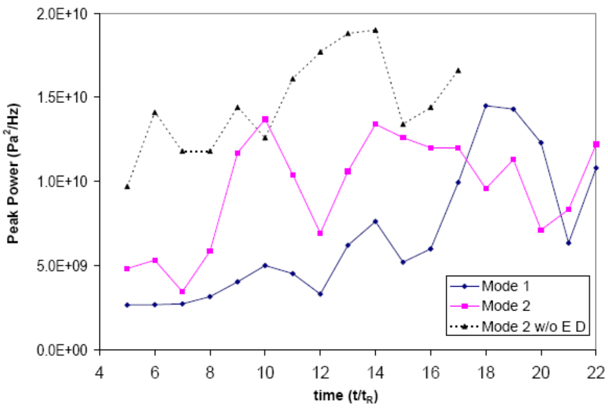

Figure 10. Peak Powers of the Power Spectrum

CONCLUSIONS AND RECOMMENDATIONS FOR FUTURE WORK

The capability for reducing the resonant pressure fluctuations in supersonic flow over an open cavity with laser energy deposition is examined. This is the first study that gives us an opportunity to see the effects of energy deposition for the control of pressure oscillations in the cavity. Results indicate that energy deposition reduces the pressure fluctuations within the cavity, changing the flow structure for several Rossiter periods.

The phase, location and magnitude of energy deposition must be optimized to have the best results in terms of the reduction of pressure oscillations. The next step in this research must be to see the effects of phase, amount, location and duration of energy deposition on the structure of the cavity configuration. The limits for the reduction of resonant pressure fluctuations by energy deposition and the way they correlate to the parameters of energy deposition is another concern.

ACKNOWLEDGMENTS

This research was supported by Air Force Office of Scientific Research under Grant F49620-01-0368 managed by Dr. John Schmisseur. All computations were performed at Rutgers University.

REFERENCES

Aerosoft Inc. General Aerodynamic Simulation Program User Manual, 1996.

Aradag, S., Yan, H. Knight, D., "Energy Deposition in Supersonic Cavity Flow", AIAA Paper No. 2004-0514, January 2004.

Bauer, R. C. and Dix, R. E., Engineering Model of Unsteady Flow in a Cavity, Calspan Corp./AEDC Operations, Arnold Engineering Development Center, TR-91-17, Tullahoma, TN, Dec. 1991.

Charwat, A. F., Roos, J. N., Dewey, Jr. F. C. and Hitz, J. A., An Investigation of Separated Flows-Part I: The Pressure Field, Journal of Aero. Sciences, Vol. 28, 1961, pp. 457-470.

Hankey, W. L. and Shang, J. S., The Numerical Solution to Pressure Oscillations in an Open Cavity, AIAA 79-0136.

Heller, H. H., and Bliss, D. B., Physical Mechanism of Flow Induced Pressure Fluctuations in Cavities and Concepts for their Suppression, AIAA Paper 75-491, March 1975.

Kaufman, L. G., II, Maciulaitis, A. and Clark, R. L., Mach 0.6 to 3.0 Flows Over Rectangular Cavities, Air Force Wright Aeronautical Labs., AFWAL-TR-82-3112, May 1983.

Knight, D., Kuchinskiy, V., Kuranov, A., Sheikin, E., Survey of Aerodynamic Flow Control at High Speed by Energy Deposition, AIAA 2003-0525, 2003.

Lamp, A. M. and Chokani, N., Computation of Cavity Flows with Suppression Using Jet Blowing, Journal of Aircraft, Vol. 34, No. 4, July-August 1997.

Lazar, E., Elliott, G. Amd Glumac, N., "Control of the Shear Layer Above a Supersonic Cavity Using Energy Deposition", AIAA Journal, vol. 46., No. 12, 2987-2997, 2008.

Leu, Y. L, Dolling, D. S., Passive Control of Pressure Oscillations in Cavity Flow with Store Release, Confederation of European Aerospace Societies Forum on Wind Tunnels and Wind Tunnel Test Techniques, 1997.

Perng, S. W., Passive Control of Pressure Oscillations in Hypersonic Cavity Flow, Ph.D. Dissertation, Dept. of Aerospace Engineering and Engineering Mechanics, University of Texas at Austin, Austin, Texas, USA., 1996.

Rizzetta, D. P., Numerical Simulation of Supersonic Flow Over a Three-Dimensional Cavity, AIAA Journal, Vol. 26, No. 7, July 1988.

Rockwell, D. and Naudascher, E., Review-Self-sustaining Oscillations of Flow Past Cavities, ASME, Journal of Fluid Engr., Vol. 100, 1978, pp. 152-165.

Rossiter, J. E., Wind-Tunnel Experiments on the Flow Over Rectangular Cavities at Subsonic and Transonic speeds, A.R.C.R. \& M., No. 3438, 1964.

Shih, S. H., Hamed, A. and Yeuan J. J., Unsteady Supersonic Cavity Flow Simulations Using Coupled k-ε and Navier-Stokes Equations, AIAA Journal, Vol. 32, No. 10, December 1994.

Stallings, R. L., Plentovich, E. B., Tracy, M. B., Hemsch, M. J., Effect of Passive Venting on Static Pressure Distributions in Cavities at Subsonic and Transonic Speeds, NASA Technical Memorandum 4549, June 1994.

Unalmis, O. H., Clemens, N. T. and Dolling, D. S., Planar Laser Imaging of a Supersonic Side-Facing Cavity, AIAA-99-0297.

Unalmis, O. H., Clemens, N.T. and Dolling, D.S., Planar Laser Imaging of High Speed Cavity Flow Dynamics,'AIAA-98-0776.

Wilcox, D. C., Turbulence Modeling For CFD, DCW Industries Inc., c1993.

Yan, H., Adelgren, R., Boguszko, M., Elliott, G., Knight, D., Laser Energy Deposition in Quiescent Air, AIAA Journal, Vol. 41, No. 10, pp. 1988--1995, 2003.

Zheltovodov and Yakovlev, V., Regimes of Separated FLows in Finite-Width Cavities and Methods of Their Control, in Separated Flows and Jets: IUTAM Symposium Novosibirsk/USSR 1990, Eds. Kozlov, V, and Dovgal, A., Springer-Verlag, Berlin, 1991, pp.529-532.